

Vascular Endothelial Growth Factor C Upregulates Trans-Lymphatic Metastasis in the Murine Liver by Recruiting Bone Marrow-Derived Cells

Hiroyuki TAKAHASHI^{1),2),3),†}, Hitomi NISHINAKAMURA^{1),†}, Naoaki SAKATA^{1),2)},
Takeshi ITOH^{1),2)}, Gumpei YOSHIMATSU^{1),2)}, Taisuke MATSUOKA^{1),2),3)},
Hideaki YAMADA^{1),4)}, Satoshi HIRAKAWA⁵⁾, Suguru HASEGAWA³⁾,
Shohta KODAMA^{1),2)}

¹⁾ *Department of Regenerative Medicine & Transplantation, Faculty of Medicine, Fukuoka University, Fukuoka, Japan*

²⁾ *Center for Regenerative Medicine, Fukuoka University Hospital, Fukuoka, Japan*

³⁾ *Department of Gastroenterological Surgery, Faculty of Medicine, Fukuoka University, Fukuoka, Japan*

⁴⁾ *Department of Cardiovascular Surgery, Faculty of Medicine, Fukuoka University, Fukuoka, Japan*

⁵⁾ *Department of Dermatology, Hamamatsu University School of Medicine, Hamamatsu, Japan*

† *These authors contributed equally to this work.*

Abstract

Colorectal cancer liver metastasis (CRCLM) is a major cause of death from colorectal cancer; however, the mechanism of intrahepatic dissemination (trans-lymphatic metastasis) is not fully elucidated. It is possible that lymphangiogenesis is the mechanism of dissemination; however, this requires confirmation, especially in the liver. In this study, we attempted to clarify the mechanism using a syngeneic murine CRCLM model, focusing on vascular endothelial growth factor C (VEGFC), a major promoter of lymphangiogenesis. We confirmed 1) intrahepatic CRCLM occurs via lymphatic vessels and upregulation of lymphangiogenesis in the CRCLM-bearing liver, 2) the degree of lymphangiogenesis and CRCLM was significantly correlated with the expression of VEGFC in colorectal cancer (CRC) cells, and 3) macrophage inflammatory protein-1 α (MIP-1 α) was released from CRC cells under VEGFC stimulation and induced migration of immature bone marrow-derived cells into the liver and differentiation into macrophages, which promoted dissemination of CRCLM. From these findings, we suggest a therapeutic strategy targeting VEGFC/MIP-1 α to reduce CRCLM.

Key words: colorectal cancer, liver metastasis, lymphangiogenesis, vascular endothelial growth factor C, macrophage inflammatory protein-1 α , tumor associated macrophage

Introduction

Colorectal cancer (CRC) is a major malignant disease, especially in advanced countries¹⁾. Over 600,000 deaths a year worldwide are estimated for CRC, most of which result from metastasis rather than local advance of the primary tumor¹⁾. According to Leporrier et al, nearly 50 percent of CRC patients have synchronous or developed liver metastasis (CRCLM)²⁾. The liver is the first target

for CRC metastasis and acts as a filter to prevent cellular invasion into the lungs and brain. Therefore, management of the primary tumor and liver metastasis is important to improve the prognosis of CRC patients. Surgical resection (i.e. hepatectomy) is accepted as the most effective treatment for CRCLM^{3),4)}; however, some patients who have a bulky tumor or multiple disseminated tumors may be unsuitable for surgical treatment. In addition, CRCLM patients often relapse even after complete curative

surgical resection. Development of novel therapies are therefore needed to improve the prognosis of advanced CRC.

Management of angiogenesis is a promising strategy for CRC treatment because CRC spreads via blood vessels, seeds multiple lesions in the liver and develops as CRCLMs⁵. Bevacizumab, an anti-vascular endothelial growth factor A (VEGFA) monoclonal antibody, is a molecular targeted drug against angiogenesis, and has been used in advanced CRC. However, clinical outcomes using bevacizumab have not been satisfactory because of drug resistance or hypo-oxygenic conditions due to poor angiogenesis⁶. This clinical feedback indicates the necessity for other strategies to improve the prognosis of CRC. Targeting lymphangiogenesis is one such strategy. While trans-lymphatic metastasis is a major route of dissemination from the primary tumor^{7,8}, it has not been considered as the cause of CRCLM. Recently, however, lymphatic invasion has been observed in clinical specimens of CRCLM-bearing liver, which is an adverse prognostic factor in CRC patients^{7,9,10}. Nevertheless, the contribution of lymphangiogenesis to CRCLM remains unclear.

This study used a syngeneic murine CRCLM model to clarify whether trans-lymphatic metastasis of CRCLM occurs via lymphatic vessels and, if so, to explore the underlying mechanism, especially focusing on vascular endothelial growth factor C (VEGFC), a promoter of lymphangiogenesis^{11,12}.

Materials and Methods

Animals

Seven-week-old C57BL/6J male mice (CLEA Japan Inc., Tokyo, Japan) were housed under specific pathogen-free conditions. The mice were carefully monitored daily by the staffs completed the course in animal care, freely feed on normal diet and were not fasted before a challenge or assessment. The care of mice and experimental procedures complied with the “Principles of Laboratory Animal Care” (Guide for the Care and Use of Laboratory Animals, National Institutes of Health publication 86-23, 1985). The experimental protocol was approved by the Animal Care and Use Committee of Fukuoka University. (Approval number: 1607955).

Cell lines and establishment of CRCLM model mice

Mouse colon adenocarcinoma-38 cells (MCA38) were

purchased from National Institutes of Health (NIH, Bethesda, MD) and used as a CRC cell line. These cells are syngeneic with the C57BL/6J mouse strain. MCA38 cells were maintained in Roswell Park Memorial Institute (RPMI) 1640 medium (ThermoFisher Scientific, Waltham, MA) supplemented with 10% fetal bovine serum (FBS; ThermoFisher Scientific), 100 U/mL penicillin and 100 mg/mL streptomycin (ThermoFisher Scientific) at 37 °C in 5% CO₂ and 95% air. MCA38 cells passaged 5-8 times were harvested from near-confluent cultures. They were infused into 8-10-week-old C57BL/6J mice as a model of CRCLM (MCA38-wt group). Under general anesthesia via intramuscular injection of 30 mg/kg pentobarbital sodium, 1×10⁵ MCA38 cells in phosphate buffered saline (PBS; ThermoFisher Scientific) were infused into the portal vein in a final volume of 200 μL. As a control group, mice were similarly injected with the same volume of PBS (PBS group). Both groups were used for assessment of survival period and rate. Some mice were excluded from the cumulative survival analysis, and they were euthanized with pentobarbital sodium to collect their livers for other analyses at postoperative day (POD) 28.

Preparing VEGFC knockout and overexpression cancer cell models

To clarify the role of VEGFC in lymphangiogenesis in CRC, both VEGFC knockout and overexpression MCA38 cell lines were established. The deletion of the VEGFC gene in MCA38 cells was performed using the clustered regularly interspaced short palindromic repeats (CRISPR) /CRISPR associated protein9 (CRISPR/Cas9) system (MCA38-vegfc-ko cells). Some cells revealed no change in VEGFC gene expression despite the genetic modification. These cells were used as control cancer cells (MCA38-vegfc-ko-ctrl cells). Briefly, guide RNAs were designed to recognize the mouse VEGFC sequence and were cloned using the GeneArt CRISPR Nuclease Vector Kit (ThermoFisher Scientific). After transformation into competent *Escherichia coli* cells (Competent Quick DH5α; Toyobo, Osaka, Japan), the plasmid sequence and oligonucleotide insert was confirmed by Fasmac Inc. (Kanagawa, Japan). The constructs were introduced into MCA38 cells using FuGENE[®] HD Transfection Reagent (Promega KK, Tokyo, Japan). Two days after transfection, CD4-positive cells were sorted using human CD4 MicroBeads (MilteniBiotec, Cologne, Germany) and seeded into 96-well plates at one cell per well and

cultured. Genomic DNA was extracted from each clone and sequenced. To minimize off-target effects of CRISPR/Cas9 genome editing, multiple positions in the VEGFC coding sequence were targeted, and two different MCA38-vegfc-ko cell lines were established. The target sequences were determined using CRISPR direct software and the positions, 298-317 and 342-362 in exon 1 were selected (C2-15, C3-22, respectively). The single strand oligonucleotides used are summarized in S1 Fig.

Regarding VEGFC overexpressed-cell line, we prepared two patterns. One was MCA38-VEGFC-overexpression (MCA38-vegfc-oe), which were established using human VEGFC-C156S pcDNA. After the construct was subcloned into pcDNA3.1 (+) (ThermoFisher Scientific), the sequence was analyzed. The subcloned pcDNA vector was introduced into near-confluent MCA38-wt cells, using Lipofectamine 2000 (ThermoFisher Scientific). The cells were cultured in a selective medium supplemented with 0, 0.1, 0.5, 1, 5, 10 or 50 $\mu\text{g}/\text{mL}$ puromycin (TaKaRa Bio, Shiga, Japan). Empty vector-transfected cells were used as control cells (MCA38-vegfc-oe-ctrl). These cells were also used for protein array analysis.

The other pattern was MCA38 with treatment of recombinant human VEGFC (rhVEGFC; R&D Systems, Minneapolis, MN). At first, cell proliferation assay was performed to the MCA38 cells treated with 0, 1 or 10 ng rhVEGFC (total medium volume; 10 μL with PBS) for overnight.

These cells were subsequently screened by cancer cell proliferation assay using a Cell Counting Kit-8 (CCK-8; Dojindo Molecular Technologies, Kumamoto, Japan) and measurement of released VEGFC levels in cultured medium under 48 hours incubation using the enzyme-linked immunosorbent assay (ELISA) kit (Quantikine[®] ELISA Human VEGF-C immunoassay; R&D Systems). The genomic DNA in these cells was purified and the sequences were confirmed by Fasmac Inc. (S2 and 3 Figs).

The activity of cancer cell proliferation was analyzed by CCK-8 following the manufacturer's protocol. 5×10^4 MCA38-wt cells were cultured in 96-well plates (total medium volume; 100 μL at 37 °C and a humidified atmosphere with 5 % CO_2) for overnight. The absorbance at 0, 6, 24 and 48 hours after treatments was evaluated. Values are expressed as relative mean of absorbance against the value at 0 hour.

Treatment of colorectal cancer cell-infused mice with VEGFC

Mice infused with 1×10^5 MCA38-wt cells were treated

with rhVEGFC (R&D Systems) (MCA38-wt + rhVEGFC group) or with PBS alone (MCA38-wt + PBS group). Using a 27-gauge syringe, 100 μL PBS with or without 1 μg rhVEGFC was injected into the peritoneal space every other day from POD 1 to 10.

Anti-mouse MIP-1 α antibody treatment

Mice infused with 1×10^5 MCA38-wt cells were treated with anti-mouse MIP-1 α polyclonal antibody (R&D Systems) (MCA38-wt + anti-MIP-1 α ab group) or isotype control antibody (R&D Systems) (MCA38-wt + isotype ctrl ab group). Using a 27-gauge syringe, 100 μL PBS with 100 μg MIP-1 α neutralizing or isotype control antibody was injected into the peritoneal space every other day from POD 1 to 10.

Real-time reverse transcription polymerase chain reaction analysis

The *mip-1 α* transcripts were analyzed by real-time reverse transcription polymerase chain reaction (RT-PCR). Briefly, total RNA was extracted from whole liver tissue. Liver was homogenized with 10 mL TRIzol (ThermoFisher Scientific), and RNA purified using a PureLink[®] RNA Mini Kit (ThermoFisher Scientific). Complementary DNAs were synthesized using high-capacity complementary DNA (cDNA) reverse transcription kits (Applied Biosystems, Carlsbad, CA) and RT-PCR was performed using a LightCycler 2.0 system (Roche, Basel, Switzerland) with SYBR Green (TaKaRa Bio). Relative quantification analysis was performed with LightCycler Software Version 4.1 (Roche). The used primers were following: mouse *mip-1 α* forward: 5'-CATGACACTCTGCAACCAAGTCTTC-3', mouse *mip-1 α* reverse: 5'-GAGCAAAGGCTGCTGGTTTCA-3', mouse *rplp0* forward: 5'-GGCAGCATTATAACCCTGAAGTG-3', mouse *rplp0* reverse: 5'-TGTACCCATTGATGATGGAGTGTG-3'.

Protein array

Upregulation of proteins in MCA38 cells stimulated with VEGFC was evaluated using a mouse angiogenesis array kit (Proteome Profiler Array; R&D Systems). Protein expression patterns were compared among MCA38-vegfc-ko, MCA38-vegfc-ko-ctrl, MCA38-vegfc-oe and MCA38-vegfc-oe-ctrl cells. Briefly, 2×10^5 cells were cultured for 48 hours (at 37°C in a humidified atmosphere with 5% CO_2). Cells were then solubilized in lysis buffer and lysates collected. They were then centrifuged at 8,000 $\times g$ for 5 minutes, and the supernatant transferred into a clean test

tube. Protein concentrations were quantified and 500 µg of protein was applied to the array membrane. Data were quantified by densitometry using ImageJ software (NIH), and values are expressed as relative mean pixel density against reference spots.

Measurement of growth factor and chemokine levels in whole liver tissue or cancer cells

VEGFC and MIP-1 α protein levels were evaluated by ELISA. To measure VEGFC levels in the liver, total protein was extracted from whole liver tissue of CRCLM and control (PBS only) mice. Liver samples were harvested, homogenized in 10 mL PBS supplemented with a protein inhibitor cocktail tablet (cOMplete ULTRA Tablets, Mini, EDTA-free, EASYpack; Sigma-Aldrich, St. Louis, MO) at 4 °C for 5 minutes using a homogenizer (T 10 basic ULTRA-TURRAX®; IKA, Staufen, Germany), and then centrifuged at 8,000 \times g for 15 minutes. The supernatant was collected and tested for the presence of VEGFC using a Quantikine® Human VEGF-C ELISA (R&D Systems). Total protein levels were also measured using a bicinchoninic acid (BCA) protein assay (ThermoFisher Scientific). Values are expressed as mean VEGFC levels relative to total protein levels.

The levels of VEGFC released by MCA38 cells were also evaluated using the Quantikine® Human VEGF-C ELISA (R&D Systems). Briefly, 1 \times 10⁶ CRC cells cultured in 1 mL of medium in 6-well plates were collected at 24 hours after seeding and tested for the presence of VEGFC. Values are expressed as mean \pm SD VEGFC protein levels.

MIP-1 α released by MCA38-wt cells was also evaluated by ELISA. 2.5 \times 10⁵ MCA38-wt cells were seeded in 6-well plates in 1 mL culture medium and incubated overnight. The medium was then removed, cells washed twice with PBS, and 1 mL culture medium excluding FBS was added to each well (serum starvation culture). 100 ng rhVEGFC dissolved in 100 µL PBS was added to three of the six wells, and 100 µL PBS alone was added to the other three wells as controls. At 6, 24 and 48 hours after incubation, media were collected and MIP-1 α levels evaluated using a Quantikine® Mouse CCL3/MIP-1 α ELISA (R&D Systems). Values are expressed as mean \pm SD MIP-1 α protein levels.

Histological examination

Liver samples were fixed in 10% formaldehyde solution for 24 hours and embedded in paraffin. All samples were

cut into 3 µm thick sections and hematoxylin-eosin (H&E) and immunofluorescence staining were performed. Post-fixation in zinc formalin and heat-induced epitope retrieval was performed on all slides. For immunofluorescence analysis, after blocking, sheep polyclonal anti-von Willebrand Factor (vWF; Abcam, Tokyo, Japan) to detect blood vessels, purified hamster anti-podoplanin (Pdp; BioLegend, San Diego, CA) and rabbit polyclonal anti-lymphatic vessel endothelial hyaluronan receptor-1 (LYVE-1; Relia Tech, Wolfenbüttel, Germany) to detect lymphatic vessels, were used as primary antibodies. Anti-vWF and anti-Pdp antibodies were diluted 1:100, and anti-LYVE-1 antibody was diluted 1:4,000 in PBS containing 5% skimmed milk and 10% serum. CyTM3-conjugated F (ab')₂ fragment donkey anti-sheep IgG (H+L) antibody (Jackson Immunoresearch, Baltimore Pike, PA), Alexa Fluor 546-conjugated whole chain goat anti-hamster IgG (H+L) antibody (ThermoFisher Scientific), and CyTM3-conjugated F (ab')₂ fragment goat anti-rabbit IgG F (ab')₂ antibody (Jackson Immunoresearch) were used as secondary antibodies for vWF, Pdp and LYVE-1, respectively. All slides were incubated with 4,6'-diamidino-2-phenylindole (DAPI) for nuclear staining. Images were acquired using a fluorescence microscope BZ-X700 (Keyence, Itasca, IL).

The numbers of intra-/extra-CRCLM blood and lymphatic vessels were counted in 10 randomly chosen images (900 \times 1,200 µm) per slide. The definitions of blood and lymphatic vessels were complete lumen structures more than 10 µm in diameter and vWF-positive, or LYVE-1 and/or Pdp positive, respectively. Values are expressed as the mean \pm SD of total vessel numbers per 10 images.

Flow cytometric cell sorting and microarray analysis

To assess the role of macrophages in the liver on lymphangiogenesis, intrahepatic macrophages were collected by cell sorting and their gene expression assessed using microarray analysis. Liver tissue without tumors was dissected at POD 28, and mechanically minced to acquire single cells. The single cells were labeled with a phycoerythrin (PE) -rat anti-mouse F4/80 antibody (BD Bioscience, Franklin lakes, NJ) and fluorescein isothiocyanate (FICT)-rat anti-CD11b antibody (BD Bioscience) to distinguish macrophages and monocytes. The suspended cells were analyzed using a BD FACS Verse (BD Bioscience) and data analysis was performed using FlowJo software (BD Bioscience).

Macrophages were acquired from F4/80⁺CD11b⁺

cells and F4/80⁺ CD11b⁺ cells treated with anti-MIP-1 α antibody or isotype control antibody using a FACS Aria Fusion Cell Sorter (BD Bioscience). Total RNA was prepared and cDNA was amplified and labeled using a Quick Amp Labeling Kit (Agilent Technologies, Santa Clara, CA). The cDNA was then hybridized to a 60K 60-mer oligomicroarray (SurePrint G3 Mouse Gene Expression Microarray 8x60K Kit; Agilent Technologies). Probes for lymphangiogenesis-related genes were extracted and they had the "P" flag in at least one sample. Heat maps were generated using R software with a hierarchical clustering method. The color indicates the log₂-transformed distance from the median of each probe. The criteria for gene regulation were defined as follows; Z-score ≥ 2.0 and ratio ≥ 1.5 for upregulated genes, and Z-score ≤ -2.0 and ratio ≤ 0.66 for downregulated genes. Microarray data analysis was supported by Cell Innovator Inc. (Fukuoka, Japan, <https://www.cell-innovator.com>). Our data have been uploaded to the Gene Expression Omnibus database (accession number: GSE113235).

Statistical analysis

Cumulative survival rates were analyzed by Kaplan-Meier methods and the Log-rank test using the SPSS 22 statistical software package (International Business Machines Corporation, 2013, NY). All data were statistically assessed by one-way analysis of variance, followed by Student's *t* test to compare two groups. *P*-values less than 0.05 were considered statistically significant.

Results

Lymphangiogenesis is upregulated in the liver bearing colorectal cancer metastases and is promoted by VEGFC.

No mice died in the PBS group; in contrast, all mice in the MCA38-wt group were dead by POD 35 (median survival period was 33 days vs. 60 days, $p = 0.001$, Fig 1A). In the MCA38-wt group, livers at POD 28 had multiple white nodules, which we considered to be liver tumors (Fig 1B-a). In contrast, there were no liver tumors in the PBS group (Fig 1B-b). Liver weight was significantly increased in the MCA38-wt group at POD 28 (2.7 ± 0.2 g vs. 1.4 ± 0.01 g, $p < 0.001$, Fig 1B-c). The increased weight reflected tumor progression. Incidentally, no more metastatic lesions were recognized in any other organs such as the lung.

Next, blood and lymphatic vessels in the liver were evaluated by immunofluorescence analysis. While the number of blood vessels (vWF-positive) in the liver was not different between MCA38-wt and PBS groups (45.3 ± 3.1 vessels/10 areas vs. 40.3 ± 3.8 vessels/10 areas, $p = 0.15$, Fig 1C), the number of lymphatic vessels (LYVE-1 or Pdp-positive) was significantly increased in the MCA38-wt group (LYVE-1: 80.6 ± 2.3 vessels/10 areas vs. 52.6 ± 4.9 vessels/10 areas, $p = 0.004$; Pdp: 93.3 ± 2.3 vessels/10 areas vs. 54.6 ± 4.1 vessels/10 areas, $p < 0.001$, Fig 1D). Notably, CRC cells were found inside several lymphatic vessels (Fig 1E). These results indicated that lymphatic vessels were upregulated in the CRCLM-bearing liver and that lymphatic vessels (not blood vessels) were the major route of metastatic dissemination in the liver.

The level of VEGFC protein was significantly higher in the MCA38-wt group compared with the PBS control group ($3.8 \times 10^{-7} \pm 2.4 \times 10^{-8}$ pg/mg vs. $2.9 \times 10^{-7} \pm 3.1 \times 10^{-8}$ pg/mg, $p = 0.01$, Fig 1F), indicating that VEGFC is an important factor contributing to lymphangiogenesis in the CRCLM-bearing liver.

Knockout of VEGFC downregulates lymphangiogenesis and suppresses cancer dissemination in colorectal cancer metastasis-bearing liver.

The VEGFC gene was disrupted in MCA38-wt cells without any influence on cell growth (Fig 2A-a, S2 Fig). Downregulation of VEGFC release was seen in MCA38-vegfc-ko cells, while no significant difference was observed between MCA38-wt and MCA38-vegfc-ko-ctrl cells (Fig 2A-b). Fig 2B illustrates the cumulative survival rate of mice infused with MCA38-vegfc-ko cells (MCA38-vegfc-ko group) or MCA38-vegfc-ko-ctrl cells (MCA38-vegfc-ko-ctrl group). The survival rate of the MCA38-vegfc-ko group was significantly prolonged, compared with the MCA38-vegfc-ko-ctrl group (median survival period was 54 days vs. 31 days, $p < 0.001$, Fig 2B). Surprisingly, disseminated tumors in the livers were prominently diminished and the whole liver weight was significantly decreased in the MCA38-vegfc-ko group (1.6 ± 0.1 g vs. 2.4 ± 0.4 g, $p < 0.001$, Fig 2C) compared with livers in the MCA38-vegfc-ko-ctrl group. While there was no difference in the number of vWF-positive blood vessels between the two groups (36.7 ± 3.5 vessels/10 areas vs. 40.7 ± 3.5 vessels/10 areas, $p = 0.24$, Fig 2D), the numbers of lymphatic vessels labeled with LYVE-1 or Pdp were significantly decreased in the MCA38-vegfc-ko group (LYVE-1: 49.3 ± 5.8 vessels/10 areas vs. 68.0 ± 2.0 vessels/10

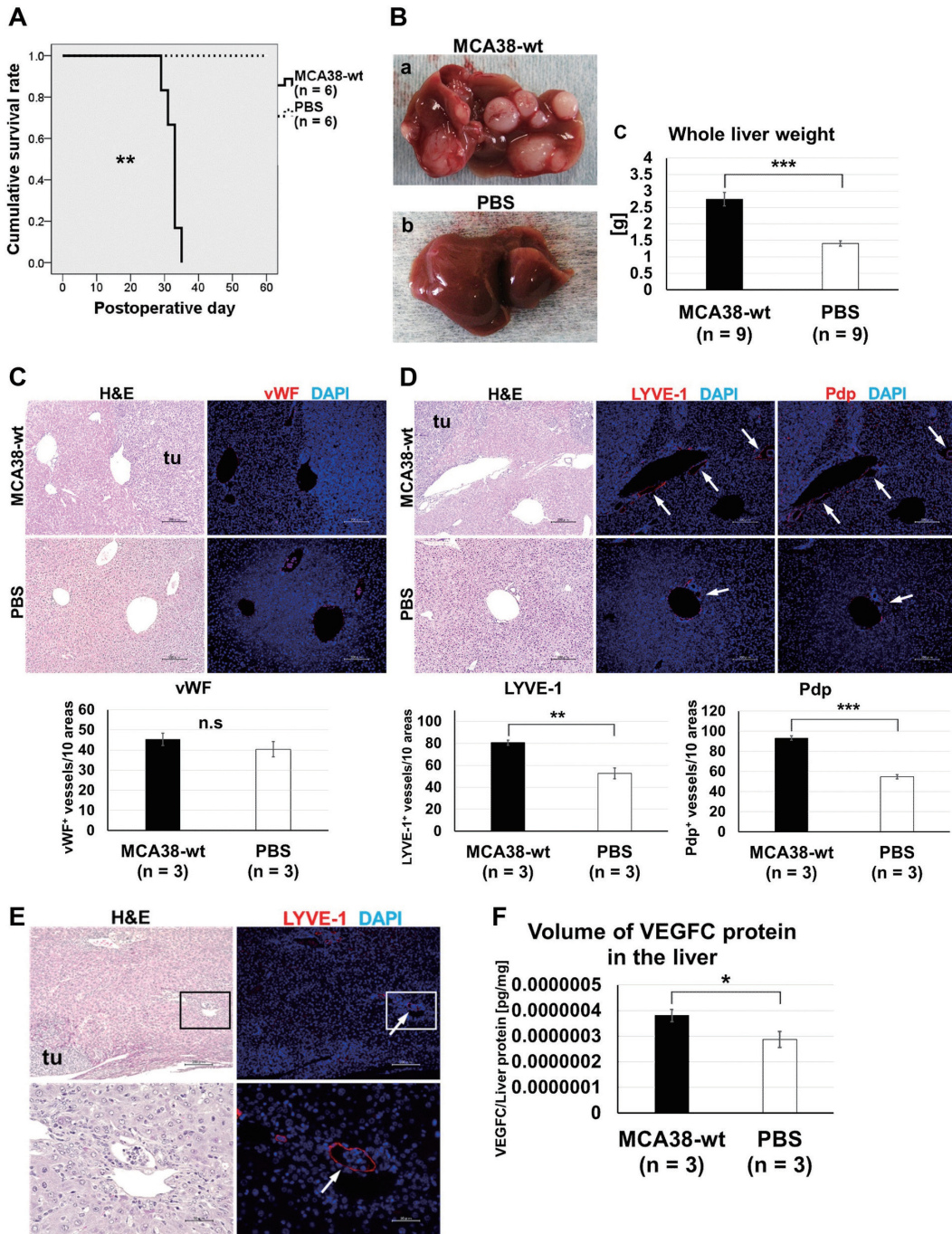


Fig. 1 Lymphangiogenesis and VEGFC are upregulated in the colorectal cancer metastasis-bearing liver.

(A) Kaplan-Meier survival curve of mice in the MCA38-wt and PBS groups. (B) The gross appearance (a, b) and whole liver weight (c) of mice autopsied at POD 28. Whole liver weight is expressed as the mean \pm SD. (C) H&E staining (left) and immunofluorescence for von Willebrand factor (vWF, right) of liver samples autopsied at POD 28. Blood vessels are recognized as vWF-positive complete lumen structures more than 10 μ m in diameter (red) with 4,6'-diamidino-2-phenylindole (DAPI)-stained nuclei (blue) as background. Bar = 200 μ m, tu = tumor. Quantitative analysis of blood vessels is shown in the graph below. The total number of blood vessels in 10 randomly chosen areas (900 \times 1,200 μ m) was counted. (D) H&E stainings (left) and immunofluorescence for lymphatic vessel endothelial hyaluronan receptor-1 (LYVE-1, middle) and podoplanin (Pdp, right) of liver samples autopsied at POD 28. Arrows indicate lymphatic vessels. Lymphatic vessels are recognized as LYVE-1- or Pdp-positive complete lumen structures more than 10 μ m in diameter (red) with DAPI-stained nuclei (blue) as background. Bar = 200 μ m, tu = tumor. Quantitative analysis of lymphatic vessels is shown in the graph below. The total number of lymphatic vessels in 10 randomly chosen areas (900 \times 1,200 μ m) was counted. (E) H&E stainings (left) and immunofluorescence for LYVE-1 (right) of liver samples autopsied at POD 28 in the MCA38-wt group. Arrows indicate MCA38-wt cell intra-lymphatic vessel lumens. Bar = 200 μ m (upper), 50 μ m (lower), tu = tumor. (F) The amount of VEGFC protein in the whole murine liver autopsied at POD 28. Values are relative to total protein amount in whole liver. * $p < 0.05$, ** $p < 0.01$, *** $p < 0.001$. All the data are expressed as means \pm SD.

areas, $p = 0.02$; Pdp: 57.0 ± 7.0 vessels/10 areas vs. 90.6 ± 7.2 vessels/10 areas, $p = 0.004$, Fig 2E). The level of VEGFC protein in the liver was also significantly lower in the MCA38-vegfc-ko group compared with the MCA38-vegfc-ko group ($1.9 \times 10^{-7} \pm 2.6 \times 10^{-8}$ pg/mg vs. $2.5 \times 10^{-7} \pm 1.7 \times 10^{-8}$ pg/mg, $p = 0.04$, Fig 2F). These data indicated that lymphangiogenesis and subsequent cancer dissemination by CRC cells were suppressed by downregulation of VEGFC.

VEGFC upregulates lymphangiogenesis and cancer dissemination in colorectal cancer metastasis-bearing liver.

We first performed CRC cell infusion using MCA38-vegfc-oe cells to clarify the role of VEGFC in lymphangiogenesis and progression of CRCLM (S3 and S4A Figs). However, this treatment produced no change in survival rate, tumor formation, angiogenesis or lymphangiogenesis (S4B, C, D and E Figs). We considered that this cell line did not secrete sufficient VEGFC to promote lymphangiogenesis or the produced VEGFC did not have biological activity; therefore, we changed to treatment with rhVEGFC for this examination.

Treatment with rhVEGFC did not affect cell growth (Fig 3A). The survival rate in the MCA38-wt + rhVEGFC group was significantly shortened compared with the MCA38-wt + PBS group (median survival period was 31 days vs. 35 days, $p = 0.001$, Fig 3B). The increase in disseminated liver tumors and increase in liver weight became more remarkable in the MCA38-wt + rhVEGFC group (2.8 ± 0.2 g vs. 2.2 ± 0.4 g, $p < 0.001$, Fig 3C). While there was no difference in the number of vWF-positive blood vessels between the two groups (45.0 ± 6.2 vessels/10 areas vs. 45.3 ± 3.1 vessels/10 areas, $p = 0.93$, Fig 3D), the number of lymphatic vessels labeled with LYVE-1 or Pdp was significantly increased in the MCA38-wt + rhVEGFC group (LYVE-1: 91.3 ± 1.2 vessels/10 areas vs. 80.3 ± 2.3 vessels/10 areas, $p = 0.006$; Pdp: 105.0 ± 4.1 vessels/10 areas vs. 92.3 ± 0.5 vessels/10 areas, $p = 0.03$, Fig 3E). The levels of VEGFC protein in the liver were also significantly higher in the MCA38-wt + rhVEGFC group ($8.2 \times 10^{-7} \pm 8.9 \times 10^{-8}$ pg/mg vs. $4.2 \times 10^{-7} \pm 1.2 \times 10^{-8}$ pg/mg, $p = 0.01$, Fig 3F). These data indicated that lymphangiogenesis and subsequent cancer dissemination were upregulated in the CRCLM-bearing liver under conditions of high VEGFC levels.

VEGFC induces MIP-1 α in colorectal cancer cells.

A protein array analysis revealed that several proteins that contribute to angiogenesis were upregulated in MCA38-vegfc-oe cells (Fig 4A). Among these proteins, the levels of MIP-1 α and C-C motif chemokine ligand 3 were the most prominent in MCA38-vegfc-oe cells compared with MCA38-vegfc-ko cells (approximately 400-fold, Fig 4B). ELISA analysis revealed that the levels of MIP-1 α induced in MCA38-wt cells were significantly upregulated after rhVEGFC stimulation in comparison with PBS-treated cells (at 48 hours: 33.3 ± 2.6 pg/mL vs. 27.4 ± 1.0 pg/mL, $p = 0.04$, Fig 4C). These results indicated that administration of VEGFC resulted in increased MIP- α secretion from CRC cells, which did not result from cellular proliferation.

Blocking MIP-1 α reduces colorectal cancer liver metastasis by compromising recruitment of bone marrow derived cells.

RNA levels of MIP-1 α were significantly upregulated in the liver in the MCA38-wt group, compared with the PBS group (2.2 ± 0.5 vs. 1.0 ± 0.3 , $p = 0.02$, Fig 5A). To clarify that MIP-1 α contributes to lymphangiogenesis and CRCLM dissemination in the liver, and to validate MIP-1 α as a therapeutic target, mice bearing CRCLM were treated with an MIP-1 α neutralizing antibody (MCA38wt + anti-MIP-1 α ab group) or an isotype control antibody (MCA38-wt + isotype ctrl ab group). Disseminated tumors in the liver were considerably diminished and whole liver weight was significantly decreased in the MCA38-wt + anti-MIP-1 α ab group (1.6 ± 0.1 g vs. 2.2 ± 0.4 g, $p = 0.01$, Fig 5B) compared with the MCA38-wt + isotype ctrl ab group.

MIP-1 α is a chemokine released by macrophages and has the potential to recruit myeloid cells derived from bone marrow, such as monocytes¹³. Therefore, we isolated and analyzed liver mononuclear cells, including macrophages and monocytes. The population of F4/80⁺ CD11b⁺ cells (defined as macrophages in the liver) was prominently upregulated in the MCA38-wt + isotype ctrl ab group compared with healthy mice (68.2% vs. 28.5%, Fig 5C middle). These results indicated that the CRCLM-bearing liver contained an increased number of macrophages that we consider to be tumor associated macrophages (TAMs).

However, the F4/80⁺ CD11b⁺ TAM population was only slightly different between the MCA38-wt + anti-MIP-1 α ab and MCA38-wt + isotype ctrl ab groups (62.7% vs. 68.2%, Fig 5C middle). Moreover, the F4/80⁺ CD11b⁺

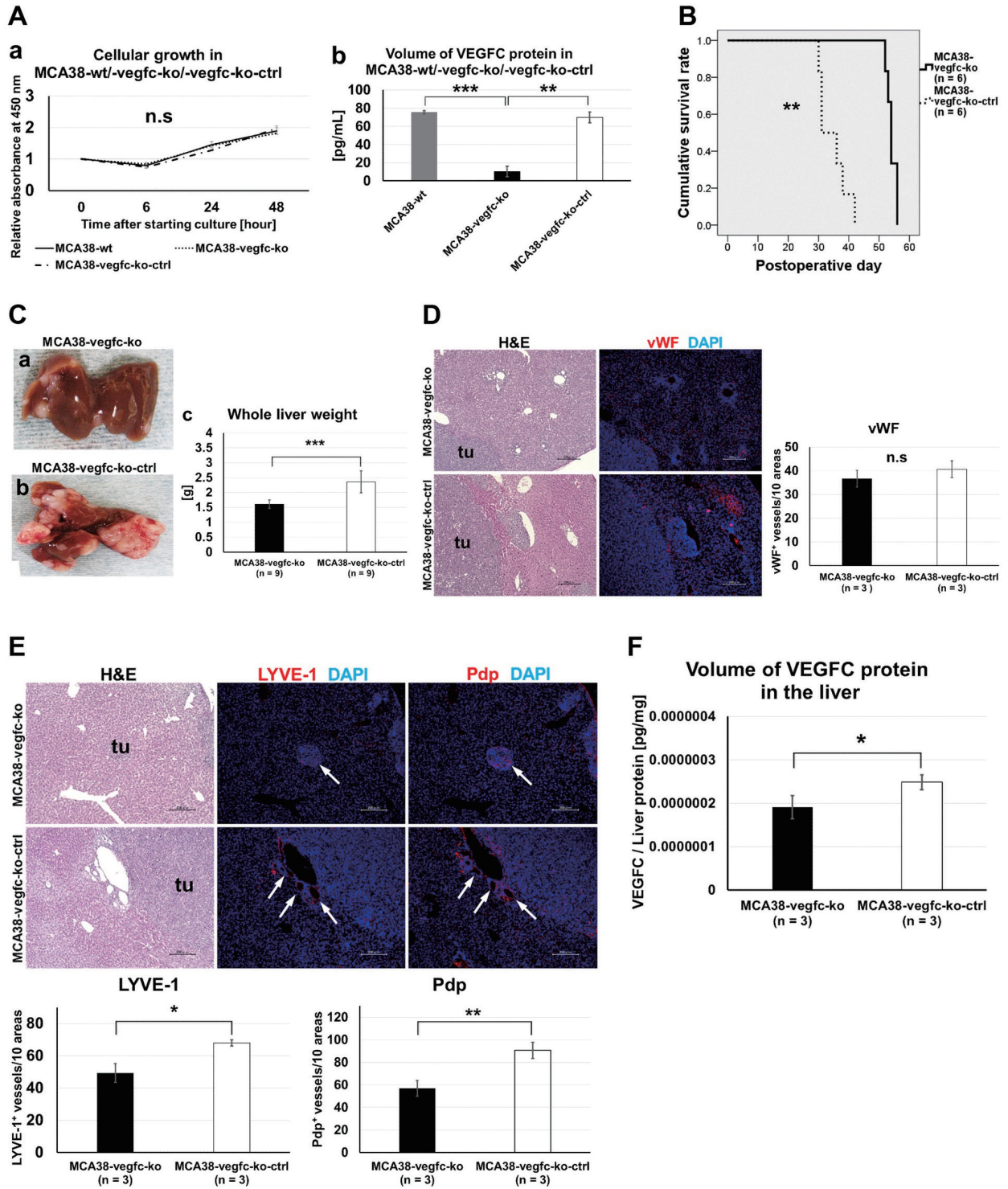


Fig. 2 Mice bearing CRCLM derived from MCA38-vegfc-ko cells show significantly downregulated lymphangiogenesis and metastasis.

(A) The growth of MCA38-wt, MCA38-vegfc-ko and MCA38-vegfc-ko-ctrl cells (a) and released VEGFC protein levels of the three kinds of the cells (b). (B) Kaplan-Meier survival curve of MCA38-vegfc-ko and MCA38-vegfc-ko-ctrl groups. (C) The gross appearance (a, b) and whole liver weight (c) of mice autopsied at POD 28. (D) H&E stainings (left) and immunofluorescence for vWF (middle) of liver samples autopsied at POD 28. Bar = 200 μ m, tu = tumor. (E) H&E stainings (left) and immunofluorescence for LYVE-1 (middle) and Pdp (right) of liver samples autopsied at POD 28. Arrows indicate lymphatic vessels. Bar = 200 μ m, tu = tumor. (F) The amount of VEGFC protein in the whole murine liver autopsied at POD 28. * $p < 0.05$, ** $p < 0.01$, *** $p < 0.001$. All the data are expressed as the means \pm SD.

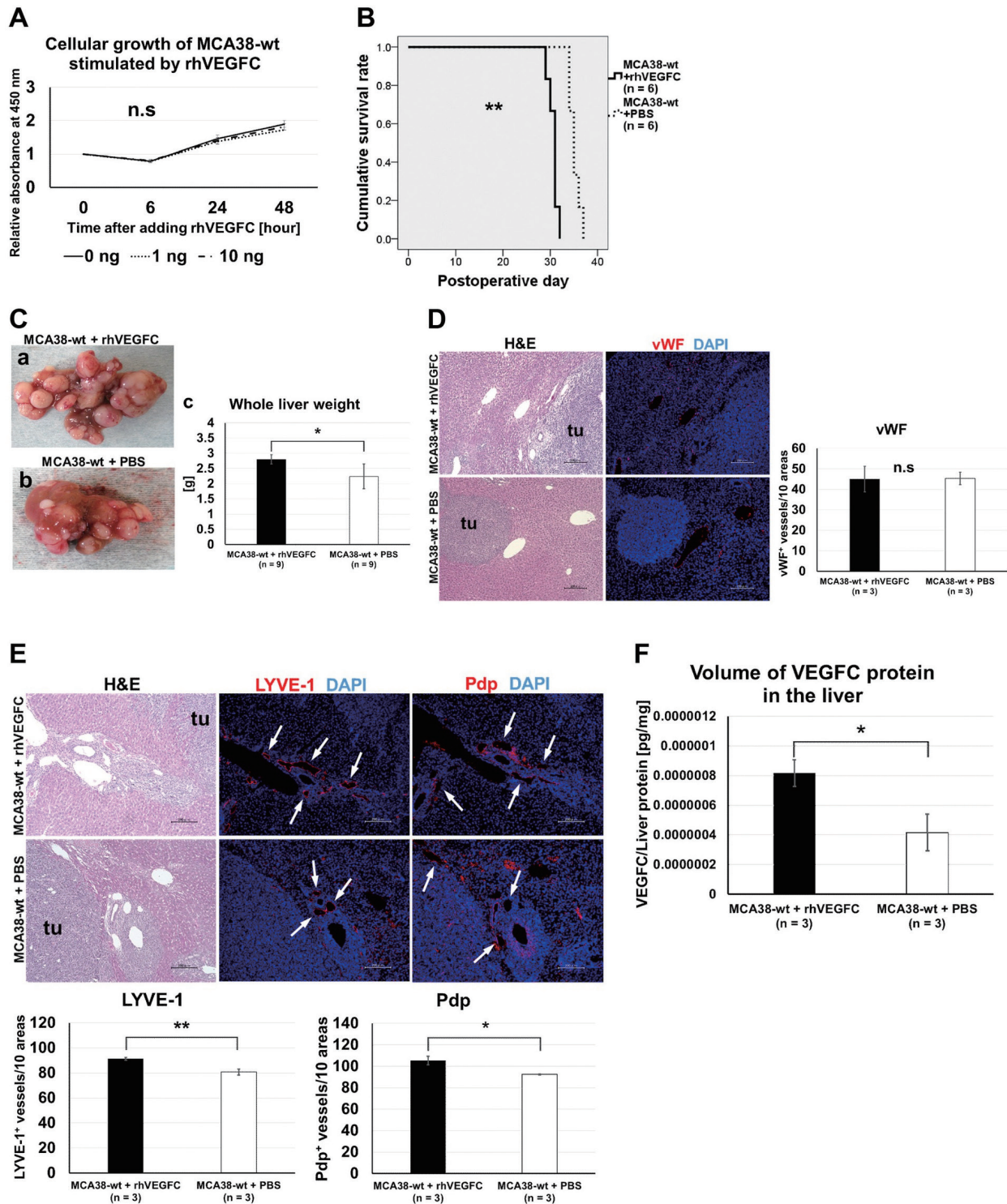


Fig. 3 Mice bearing CRCLM treated with recombinant human VEGFC show significantly upregulated lymphangiogenesis and metastasis.

(A) Growth of MCA38-wt cells stimulated by recombinant human VEGFC (rhVEGFC). Values at each time point are expressed as the absorbance at 450 nm relative to that at 0 hour. (B) Kaplan-Meier survival curve of MCA38-wt + rhVEGFC and MCA38-wt + PBS groups. (C) The gross appearance (a, b) and whole liver weight (c) of mice autopsied at POD 28. (D) H&E stainings (left) and immunofluorescence for vWF (middle) of liver samples autopsied at POD 28. Bar = 200 μ m, tu = tumor. Quantitative analysis of blood vessels is shown in the graph (right). (E) H&E stainings (left) and immunofluorescence for LYVE-1 (middle) and Pdp (right) of liver samples autopsied at POD 28. Arrows indicate lymphatic vessels. Bar = 200 μ m, tu = tumor. (F) The amount of VEGFC protein in the whole murine liver autopsied at POD 28. * $p < 0.05$, ** $p < 0.01$. All the data are expressed as the means \pm SD.

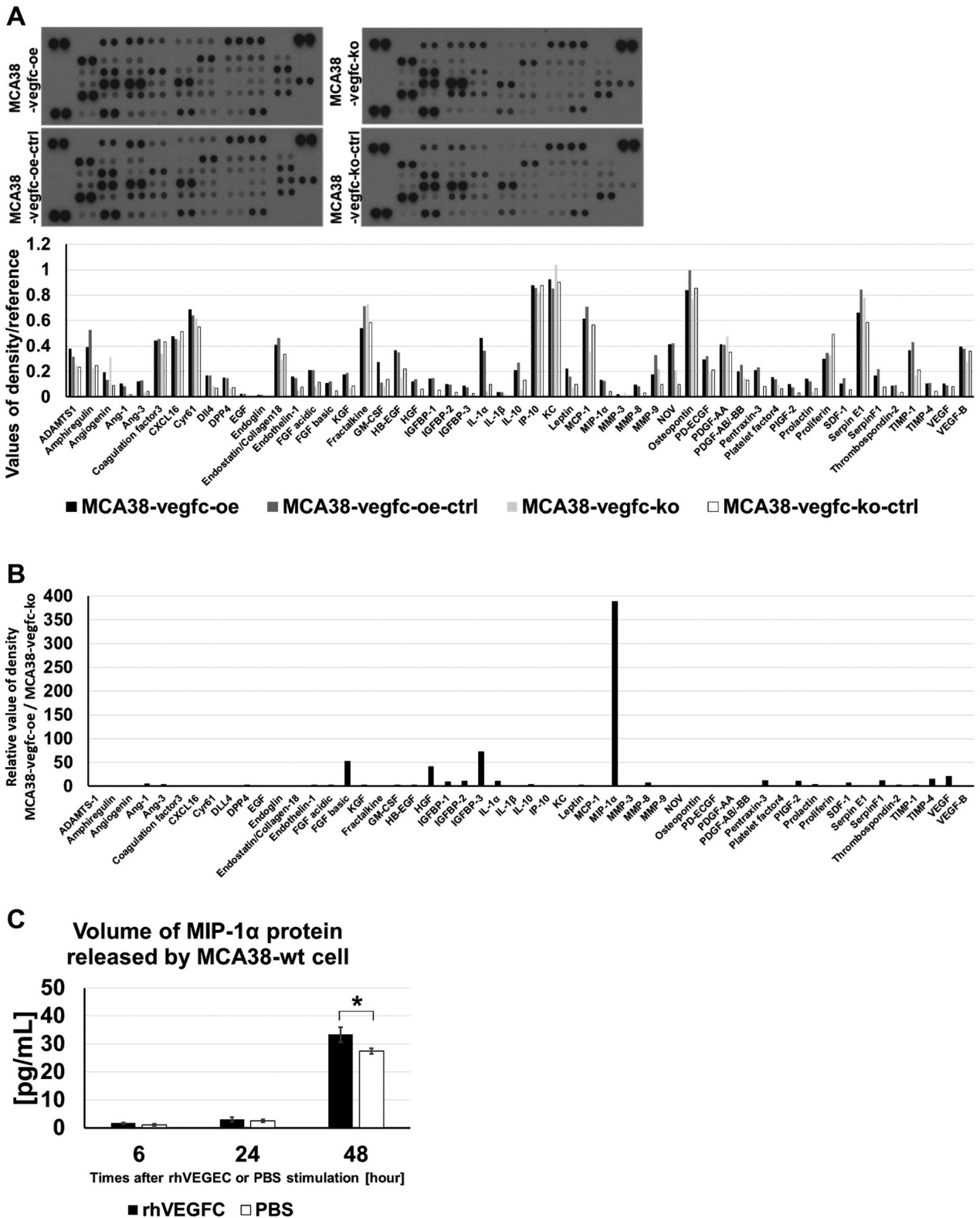


Fig. 4 MIP-1 α is upregulated in CRC cells stimulated by VEGFC. (A) A protein array analysis was performed on MCA38-vegfc-ko cells, MCA38-vegfc-ko-ctrl cells, MCA38-vegfc-oe cells and MCA38-vegfc-oe-ctrl cells. Raw data is shown in the upper panel. Values are expressed as relative mean pixel density against reference spots (lower panel). (B) Comparison of MCA38-vegfc-oe cells with MCA38-vegfc-ko cells. Values are expressed as the relative mean pixel density of MCA38-vegfc-oe cells relative to the density of MCA38-vegfc-ko cells. (C) The amount of MIP-1 α in MCA38-wt cells stimulated by 100 ng rhVEGFC or PBS at 6, 24 and 48 hours. Values are expressed as means \pm SD of three independent experiments of three replicates. * $p < 0.05$.

cells consist of two populations classified by the F4/80 ratio (F4/80^{low} and F4/80^{high} CD11b⁺ TAMs). Microarray analysis revealed no significant change in gene expression was associated with lymphangiogenesis in F4/80⁺ CD11b⁺ TAMs among the groups (S5 Fig). However, the F4/80^{low} CD11b⁺ TAM population (defined as differentiated macrophages from bone marrow derived cells) was different in the MCA38-wt + anti-MIP-1 α ab group compared with the MCA38-wt + isotype ctrl ab group (35.1% vs. 49.8%, Fig 5C right). These results indicated that the MIP-1 α neutralizing antibody suppressed the promotion of myeloid cells from bone marrow that have the potential to differentiate into TAMs, and resulted in diminished metastasis in the CRCLM liver.

Discussion

CRCLM contributes to the less favorable outcomes of CRC¹, and thus, management of CRCLM is important to improve prognosis of CRC patients. Suppression of tumor-derived angiogenesis is a possible treatment strategy, but it would be difficult to prevent CRCLM by suppressing angiogenesis because CRCLM is usually a hypovascular tumor and is surrounded by a fibrous capsule¹⁴. Therapies targeting angiogenesis have minimal effect at diminishing CRCLM tumors and have the disadvantage of inducing hypo-oxygenic conditions, which promotes tumor growth¹⁵. Ebos et al. reported accelerated metastasis after treatment with an inhibitor of tumor angiogenesis¹⁶.

In this study, we clarified that angiogenesis in the CRCLM-bearing liver was not upregulated and that CRC cells invaded lymphatic vessels. These findings indicate that lymphatic vessels, rather than blood vessels, are conductors of CRC dissemination in the liver. Peripheral lymphatic vessels are not surrounded by smooth muscles and the cell-cell junctions are not tight^(7,17,18). Lymphatic vessels are, therefore, leaky and tumor cells can easily migrate through the vessels. Moreover, VEGFC promotes circumferential enlargement of the collecting vessels, leading to increased lymph flow and transport of tumor cells¹⁸. We demonstrated that VEGFC in the liver was strongly expressed in the presence of CRCLM. These characteristics contribute to dissemination of CRC cells in the liver via lymphatic vessels. One study has demonstrated upregulation of lymphangiogenesis around primary CRC tumors and promotion of metastasis under the influence of VEGFC⁸; however, the role of lymphatic vessel growth in the progression of liver tumors has

been largely unknown. This study clarifies a similar phenomenon in the CRCLM-bearing liver.

Among the various immune cells, macrophages interact the most with lymphatic vessels and are accepted as a component of tumor tissues and a regulator of lymphangiogenesis^{17,19-22}. TAMs promote metastatic behaviors by inducing VEGFC and lymphangiogenesis in gastric and lung cancers^{23,24}. In our previous study in a murine model of hindlimb ischemia, CD11b⁺ myeloid cells also released VEGFC to upregulate lymphangiogenesis²⁵. In this study, the number of F4/80⁺ CD11b⁺ macrophages was prominently increased in the liver bearing CRCLM, indicating that such TAMs promote lymphangiogenesis and dissemination of CRCLM. MIP-1 α , which can promote immature bone marrow-derived cells, is induced by endotoxin-stimulated macrophages¹³. MIP-1 α is also associated with the regulation of cell growth and metastasis of different tumors²⁶⁻²⁹. Mancardi et al. reported that lymphatic endothelial cells secrete chemotactic factors, such as monocyte chemoattractant protein-1 and MIP-1 α , to attract macrophages³⁰. Here, we revealed that CRC cells also release MIP-1 α , which was auto-regulated via VEGFC stimulation, and that neutralizing MIP-1 α prominently diminished CRCLM. Accordingly, it is assumed that MIP-1 α might change the expression of genes associated with lymphangiogenesis in these TAMs.

The macrophages in the liver can be distinguished into two populations: F4/80^{high} tissue resident cells (i.e., Kupffer cells) and F4/80^{low} bone marrow-derived cells³¹⁻³³. In the anti-MIP-1 α antibody administrated liver, the population of F4/80^{low} CD11b⁺ bone marrow-derived TAMs was decreased, while the population of F4/80^{high} CD11b⁺ tissue resident TAMs was not (Fig 5C). Kim and colleagues reported that F4/80^{low} CD11b⁺ bone marrow-derived macrophages showed a greater inflammatory phenotype than F4/80^{high} CD11b⁺ tissue resident Kupffer cells in the liver³¹. Kitamura et al. suggested that reduced immature myeloid cell accumulation could suppress metastatic expansion of colon cancer in the liver³⁴. These studies indicate that immature bone marrow-derived cells might contribute more to tumor growth than mature tissue resident Kupffer cells in CRCLM-bearing liver. Moreover, the mechanism underlying the reduction of CRCLM by blocking MIP-1 α involved the suppressed recruitment of bone marrow-derived cells, not altered TAM gene expression associated with lymphangiogenesis. The hepatic macrophage-deleted mice can be more suitable

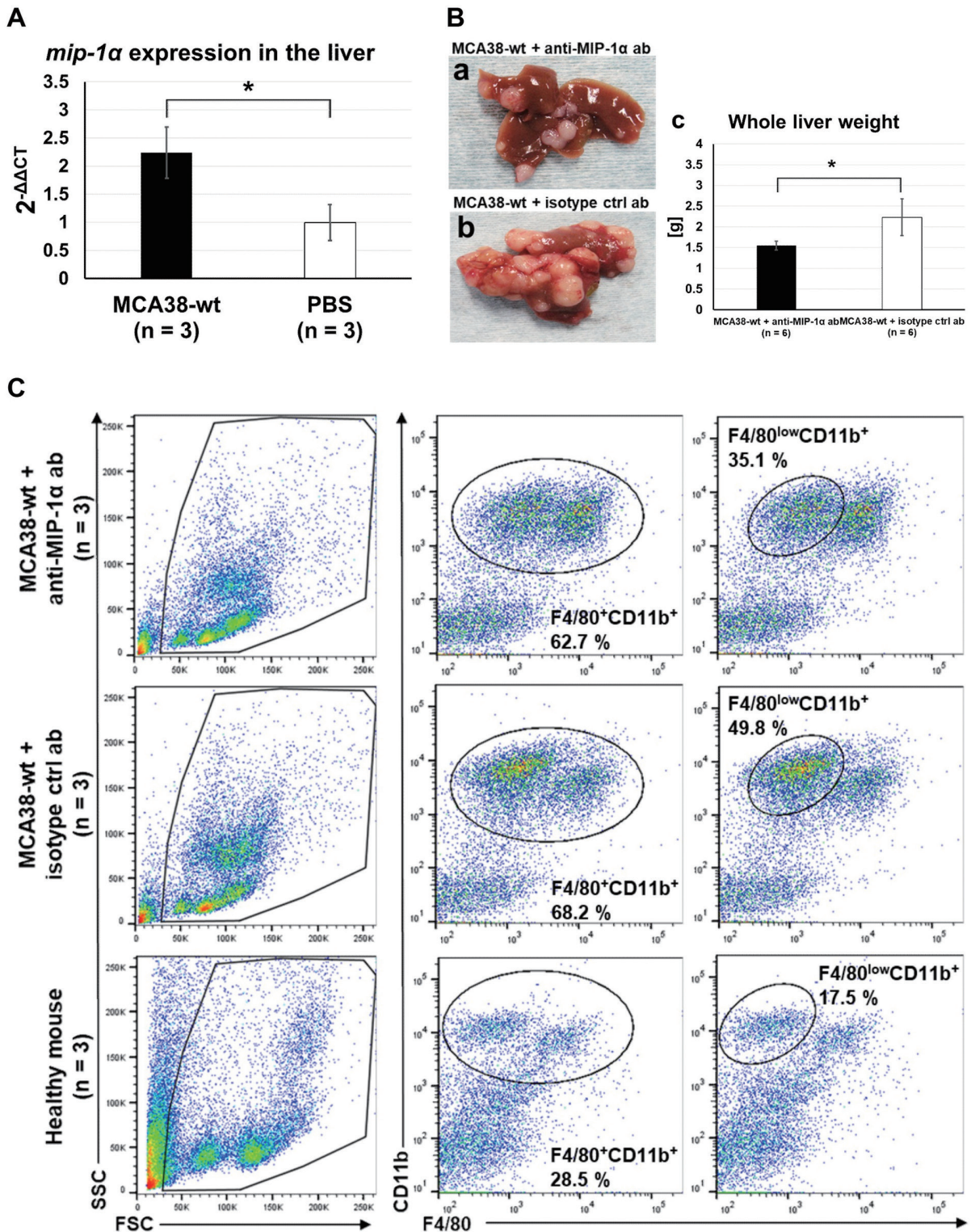


Fig. 5 Blocking MIP-1 α suppresses the promotion of bone marrow derived cells and reduces the CRCLM.

(A) RNA levels of MIP-1 α in the whole liver of mice autopsied at POD28 in MCA38-wt or PBS groups. (B) The gross appearance (a, b) and whole liver weight (c) of mice autopsied at POD 28. (C) Flow cytometry analysis of macrophages in MCA38-wt + anti-MIP-1 α ab, MCA38-wt + isotype ctrl ab, and healthy mouse groups autopsied at POD 28. Macrophages were labeled with PE-rat anti-mouse F4/80 antibody and FITC-rat anti-CD11b antibody, which are markers of mature macrophages and immature myeloid cells derived from bone marrow, respectively. The scatter diagrams for the MCA38-wt + anti-MIP-1 α ab and MCA38-wt + isotype ctrl ab groups were for cell sorting in microarray analysis (aggregation of three mice). The scatter diagrams for the healthy mouse group are representative of multiple replications. Values are expressed as a percentage of the total population. * $p < 0.05$. All the data are expressed as the means \pm SD.

models to assess the co-relationship between CRCLM and hepatic macrophages. Although we established the model using L-chlodronate liposome, it was practically difficult to continue the examination due to the lethality immediately after cancer cell infusion. However, a strategy targeting this MIP-1 α chemokine pathway has been reported in different malignancies^{35), 36)}, and this study is in accord with these previous reports. Therapies targeting VEGFC signal may be useful as a CRCLM treatment strategy because, in addition to the direct effect, downregulation of MIP-1 α suppresses the recruitment of bone marrow-derived cells, which results in differentiation into TAMs that contribute to CRCLM (Fig 6). The correlation between TAMs and lymphangiogenesis in the liver remains unclear and further research is warranted as well as to investigate hepatic bone marrow-derived cells.

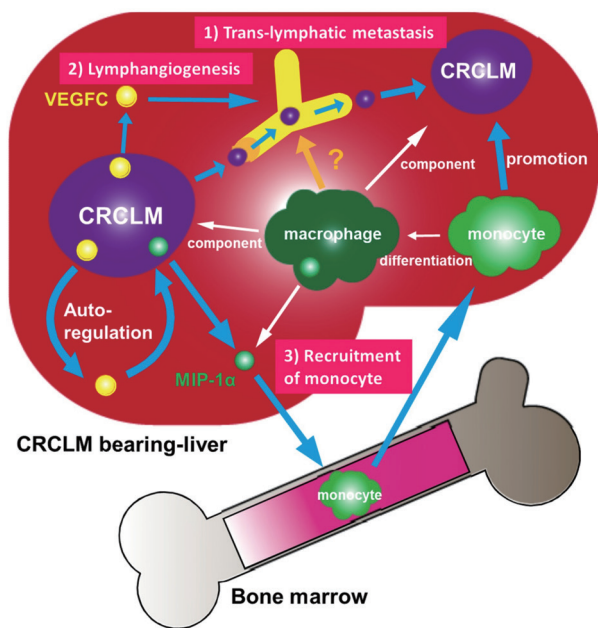


Fig. 6 Proposed mechanism underlying the effects of VEGFC in the colorectal cancer metastasis-bearing liver.

Scheme summarizing this study. 1, 2) VEGFC upregulates lymphangiogenesis and subsequent trans-lymphatic metastasis in the colorectal cancer metastasis bearing liver (CRCLM). 3) Colorectal cancer cells secrete MIP-1 α by VEGFC autoregulation, which contributes to tumor growth by recruiting bone marrow-derived cells, such as a monocytes. Whether hepatic macrophages contribute to lymphangiogenesis in the liver remains unclear.

This study has two three limitations. One is the influence of VEGFC derived from recipient mice on lymphangiogenesis of CRCLM-bearing liver. Although

VEGFC gene knockout mice are suitable for preventing this influence, VEGFC knockdown can result in death due to lymphedema^{37), 38)}. However, we consider the influence of recipient VEGFC can be excluded because there was a significant difference in lymphangiogenesis in the liver between VEGFC knockout and control CRCLMs. In other words, the VEGFC derived from CRC cells might be more important for lymphangiogenesis than that from the recipient. The other limitation is the difficulty in establishing a VEGFC overexpression cell model. The MCA38-vegfc-oe cells derived from CRCLM-bearing liver revealed unaltered lymphangiogenesis (S4 Fig). A possible reason is that the level of VEGFC produced by MCA38-vegfc-oe cells was insufficient to upregulate lymphangiogenesis, although the levels of VEGFC were significantly upregulated in cells examined *in vitro* (S4 Fig). The produced VEGFC might miss the biological activities. Therefore, we used cells treated with rhVEGFC for this examination. The rhVEGFC specifically reacts to VEGFR-3 and promotes lymphangiogenesis, so that we can exclude the efficacy of angiogenesis through the VEGFR-2 signaling pathway³⁹⁾. A preliminary experiment revealed that 5,000-10,000 pg endogenous VEGFC was present in the murine liver. CRCLM-bearing mice were treated with 0, 0.01, 0.1 or 1 μ g rhVEGFC, and only mice administrated 1 μ g rhVEGFC revealed significantly expanded CRCLM (S6 Fig). Thus, more than 100-fold higher levels of VEGFC than are present in the normal mouse liver were needed to elicit a response.

VEGFC/VEGFR-3 has been studied as a lymphangiogenic signaling pathway^{7), 11), 12), 17), 18), 40)}. Targeting this signal restricts tumor lymphangiogenesis, lymphatic enlargement and lymph node metastasis^{7), 40)-42)}. Currently, many medicines targeting lymphangiogenesis via the VEGFC receptor are clinically approved. For example, Sorafenib, Sunitinib and Regorafenib were developed for this purpose⁴³⁾⁻⁴⁶⁾. Among these drugs, Regorafenib has been approved for metastatic CRC and gastrointestinal stromal tumor. Regorafenib is the first small molecule multi-kinase inhibitor with survival benefits in metastatic CRC; however, treatment-related adverse events occur in more than 90% of patients using Regorafenib. These adverse events tend to be severe (grade three or higher)⁴⁶⁾. An anti-VEGFC antibody is considered a potential drug because of high selectivity. VGX-100 is such a VEGFC-targeting monoclonal antibody, and a phase I study (NCT01514123) has been ongoing for the treatment of advanced solid tumors^{40), 47)}.

Target gene	Forward strand oligonucleotide	Reverse strand oligonucleotide
vegfc-1 (C3)	5'-TCGAGTCGGGACTGGGCTTCGTTTT-3'	5'-GAAGCCCAGTCCCGACTCGACGGTG-3'
vegfc-2 (C2)	5'-GCTGATCCCCAGTCCGCGCGTTTT-3'	5'-CGCGCGGACTGGGGATCAGCCGGTG-3'

S1 Figure The used single strand oligonucleotides for CRISPR/Cas9.

MCA38-vegfc-ko (1; C3-22)

Guide ATGTCCGGTTTCCTGTGAGGCTCGTACCTGACACCCGGGAGCCTCTCCCCGTGAGGGCTGCCAGAGCCGAGGGCAAAGTTGC
 <M><S><G><F><L><Z><G><S><Y><L><T><P><G><S><L><S><P><V><R><A><A><R><A><E><G><K><S><C>
 C3-22

Guide GAGCCCGAGTCCCGGAGACGCTCGCCAGGGGGTCCCCGGGAGGAAACCAGGGACAGGGACCAGGAGAGGACCTCAGCC
 <E><P><P><S><P><G><R><R><S><P><R><G><V><P><G><R><K><P><R><D><R><D><Q><E><R><T><S><A>
 C3-22 CGGAGAGGACAT - AGCC

Guide TCACGCCCCAGCCTGCGCCAGCCAACGGACCGGC-CTCCCTGCTCCCGTCCATCCACCATGCACCTGCGTGTGCTTCTTGTCT
 <S><R><P><S><L><R><Q><P><T><D><R><P><P><C><S><R><S><I><H><H><A><L><A><V><L><L><V><
 C3-22 TCACGCCCCAGCCTGCGCCAGCCAACGGACCGGCAGTCCCTGCTCCCGTCCATCCACCATGCACCTGCGTGTGCTTCTTGTCT

Guide CTGGCGTGTTCCTGCTCGCCGCTGCGCTGATCCCCAGTCCGCGCGAGGGCGCCGCCACCGTCCGCGCTTCGAGTCGGGACTG
 S><G><V><F><P><A><R><R><C><A><D><P><Q><S><A><R><G><A><R><H><R><R><R><L><R><V><G><T><
 C3-22 CTGGCGTGTTCCTGCTCGCCGCTGCGCTGATCCCCAGTCCGCGCGAGGGCGCCGCCACCGTCCGCGCTTCGAGG-GAGAGTG

Guide GGCTTCTCGAAAGCGGAGCCGACGGGGCGAGGTCAAGGTAGGTGCAAGGGACCCCG
 G><L><L><G><S><G><A><R><R><G><R><G><Q><G><R><C><K><G><P><
 C3-22 GGCTTCTCGAAAGCGGAGCCGACGGGGCGAGGTCAAGGTAGGTGCAAGGGACCCCG

MCA38-vegfc-ko (2; C2-15)

Guide ATGTCCGGTTTCCTGTGAGGCTCGTACCTGACACCCGGGAGCCTCTCCCCGTGAGGGCTGCCAGAGCCGAGGGCAAAGTTGC
 <M><S><G><F><L><Z><G><S><Y><L><T><P><G><S><L><S><P><V><R><A><A><R><A><E><G><K><S><C>
 C2-15

Guide GAGCCCGAGTCCCGGAGACGCTCGCCAGGGGGTCCCCGGGAGGAAACCAGGGACAGGGAAGGAGAGGACCTCAGCC
 <E><P><P><S><P><G><R><R><S><P><R><G><V><P><G><R><K><P><R><D><R><D><Q><E><R><T><S><A>
 C2-15 GAAGGAAAGAC-TCAGCC

Guide TCACGCCCCAGCCTGCGCCAGCCAACGGACCGGCTCCCTGCTCCCG-GTCCATCCACCATGCACCTGCTGTGCTTCTTGTCTC
 <S><R><P><S><L><R><Q><P><T><D><R><P><P><C><S><R><S><I><H><H><A><L><A><V><L><L><V><S
 C2-15 TCACGCCCCAGCCTGCGCCAGCCAACGGACCGGCTCCCTGCTCCCGAGTCCATCCACCATGCACCTGCTGTGCTTCTTGTCTC

Guide TGGCGTGTTCCTGCTCGCCGCTGCGCTGATCCCCAGTCCGCGAGGGCGCCGCCACCGTCCGCGCTTCGAGTCGGGACTGG
 ><G><V><F><P><A><R><R><C><A><D><P><Q><S><A><R><G><A><R><H><R><R><R><L><R><V><G><T><G
 C2-15 TGGCGTGTTCCTGCTCGCCGCTGCGCTGATCCCCAGTCCGCGAGGGCGCCGCCACCGTCCGCGCTTCGAGTCGGGACTGG

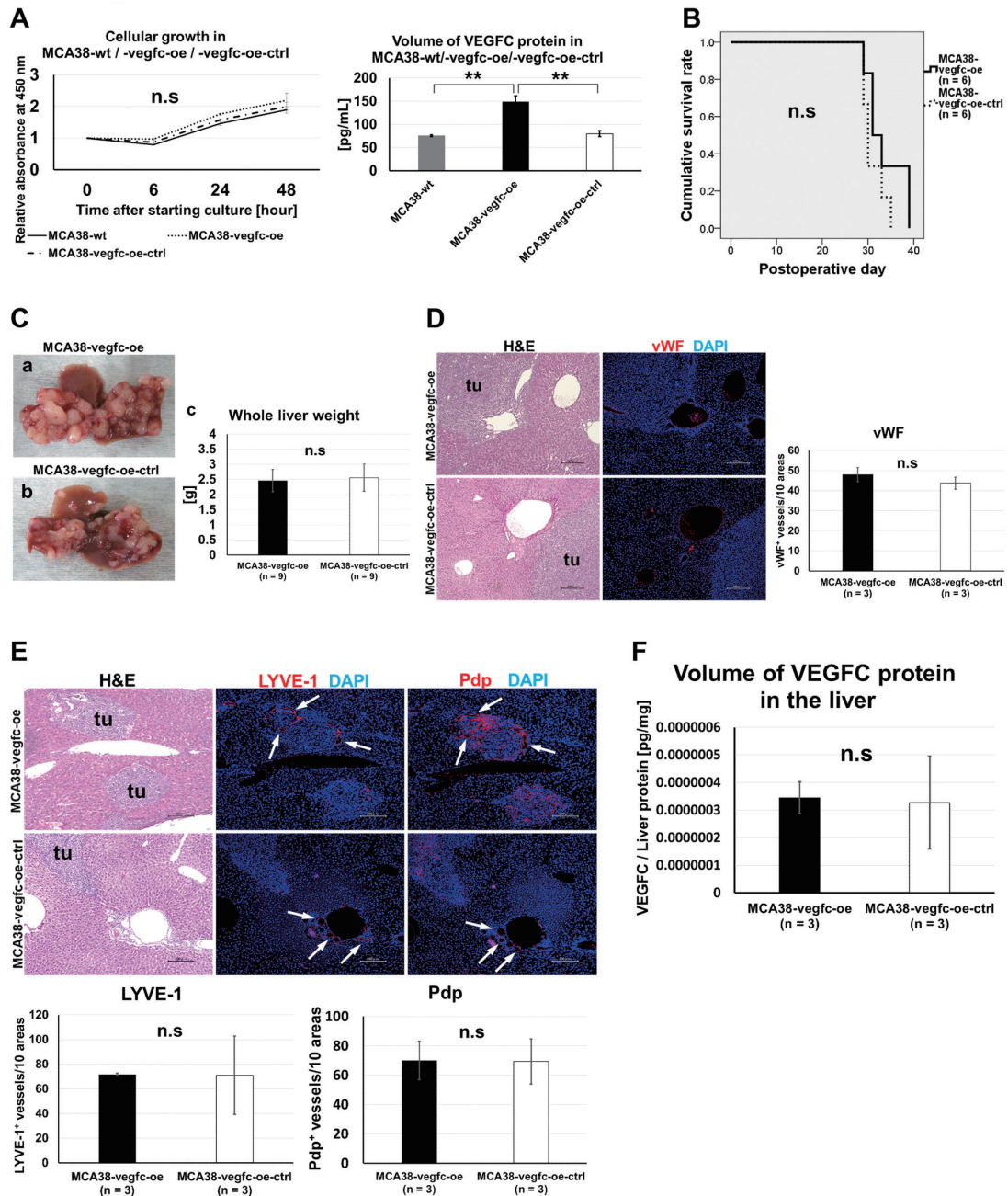
Guide GCTTCTCGAAAGCGGAGCCGACGGGGCGAGGTCAAGGTAGGTGCAAGGGACCCCG
 ><L><L><G><S><G><A><R><R><G><R><G><Q><G><R><C><K><G><P><
 C2-15 GCTTCTCGAAAGCGGAGCCGACGGGGCGAGGTCAAGGTAGGTGCAAGGGACCCCGAGA

S2 Figure Deletion of the VEGFC gene in MCA38 cells using the CRISPR/Cas9 system. CRISPR/Cas9-mediated knockout of VEGFC in MCA38-wt cells. In the VEGFC exon 1 coding sequence, positions 298-317 and 342-362 were selected for guide RNA design (C2-15, C3-22, respectively). The knockout MCA38 clone contains a deletion in the VEGFC gene causing a frameshift mutation. The VEGFC nucleotide sequences have been deposited in GenBank (accession number MN_009506.2).

guide TTTAAACCTCCATGTGTGTCCTCTACAGATGTGGGGTTGCTGCAATAGTGAGGGGCTGCAGTGCATGAACACCAGCACGAGCT
 <F><K><P><P><C><V><S><V><Y><R><C><G><G><C><C><N><S><E><G><L><Q><C><M><N><T><S><T><S>
 pniprep TTTAAACCTCCAAGTGTGTCCTCTACAGATGTGGGGTTGCTGCAATAGTGAGGGGCTGCAGTGCATGAACACCAGCACGAGCT
 miniprep TTTAAACCTCCAAGTGTGTCCTCTACAGATGTGGGGTTGCTGCAATAGTGAGGGGCTGCAGTGCATGAACACCAGCACGAGCT
 Human VEGF-C TTTAAACCTCCATGTGTGTCCTCTACAGATGTGGGGTTGCTGCAATAGTGAGGGGCTGCAGTGCATGAACACCAGCACGAGCT

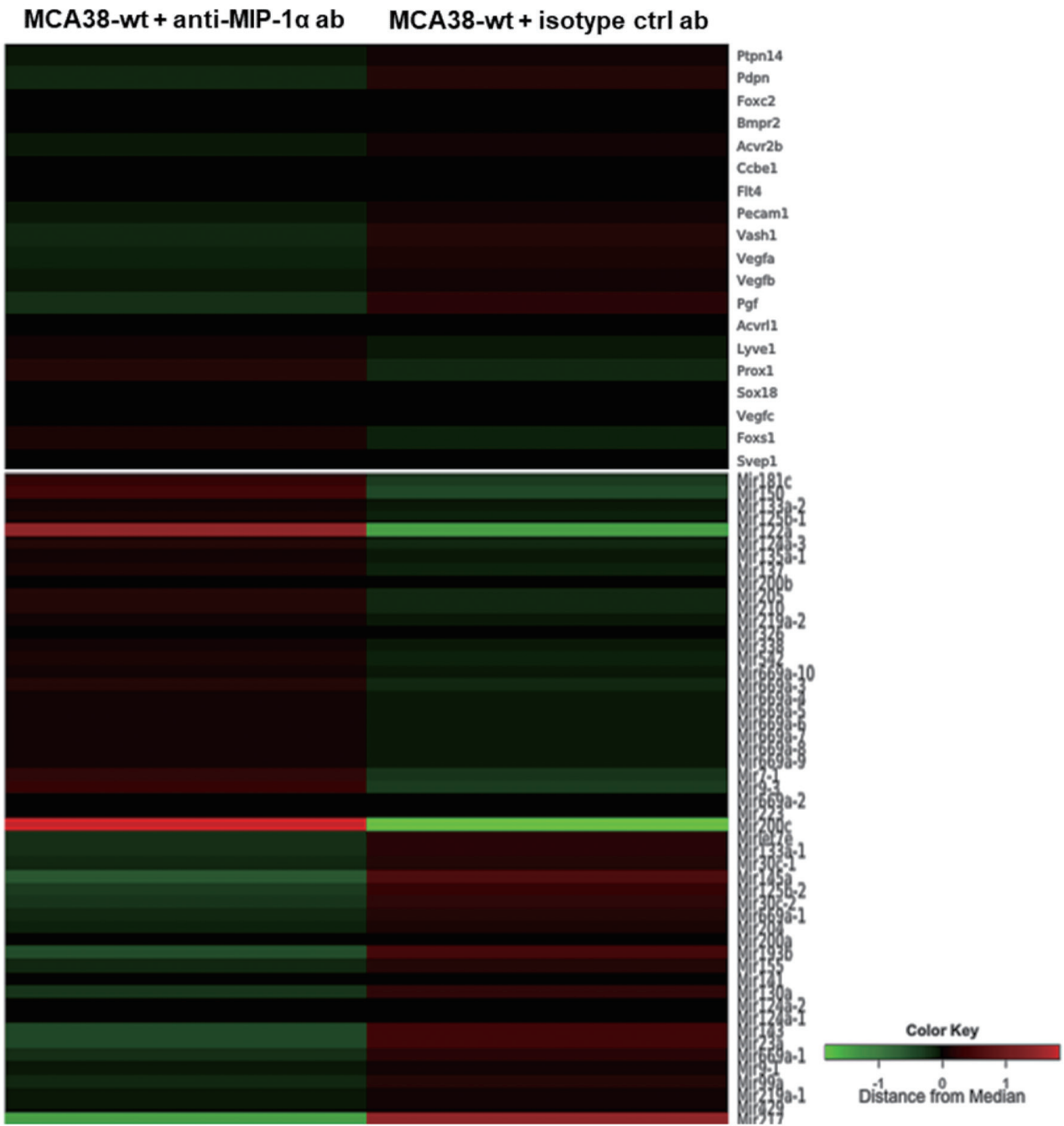
S3 Figure MCA38 cells transfected with pcDNA encoding the human VEGFC gene.

A VEGFC overexpression-cell line (MCA38-vegfc-oe) was established, using human VEGFC-C156S pcDNA. Genomic DNA sequencing confirmed Cys156 changed to Ser.



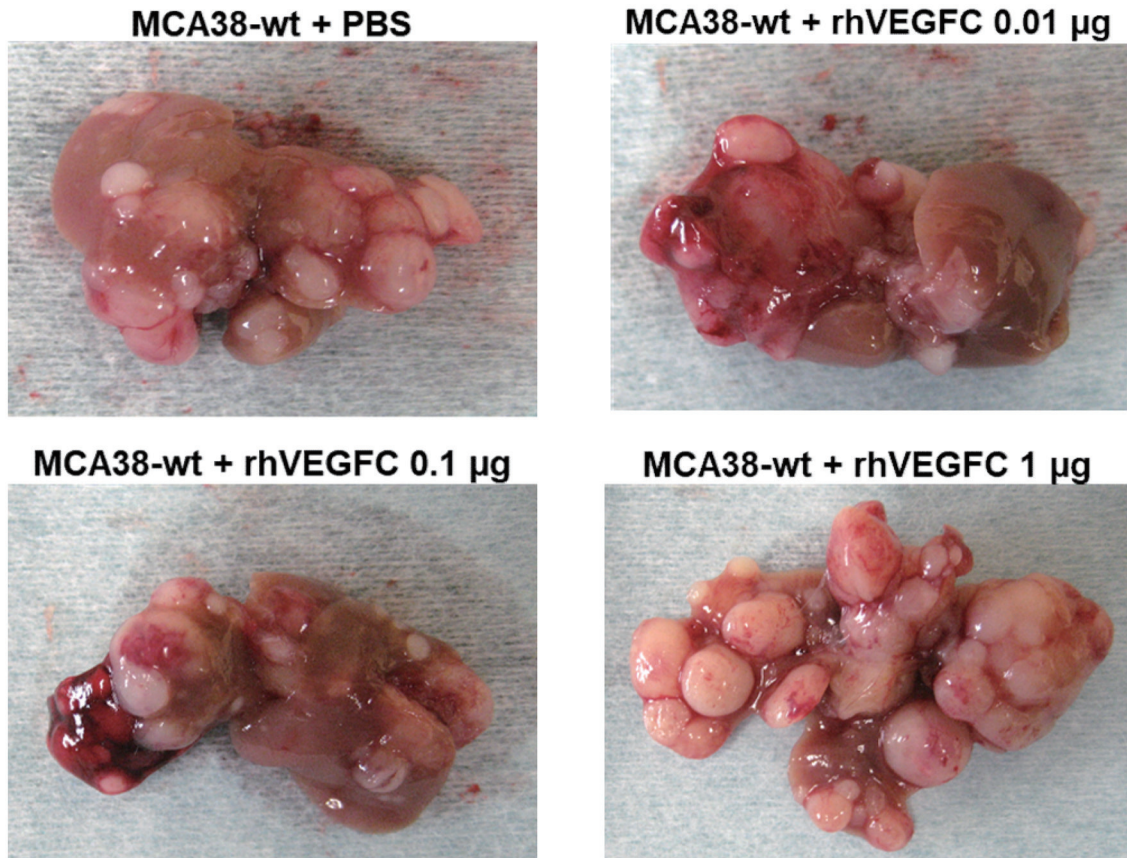
S4 Figure Mice bearing CRCLM derived from MCA38-vegfc-oe cells display no changes in lymphangiogenesis or metastasis.

(A) The cell growth of MCA38-wt, MCA38-vegfc-oe and MCA38-vegfc-oe-ctrl cells (a) and released VEGFC protein levels for the three kinds of the cells (b). (B) Kaplan-Meier survival curve of MCA38-vegfc-ko and MCA38-vegfc-ko-ctrl groups. (C) The gross appearance (a, b) and whole liver weight (c) of mice autopsied at POD 28. (D) H&E stainings (left) and immunofluorescence for vWF (middle) of liver samples autopsied at POD 28. Bar = 200 μ m, tu = tumor. (E) H&E stainings (left) and immunofluorescence for LYVE-1 (middle) and Pdp (right) of liver samples autopsied at POD 28. Arrows indicate lymphatic vessels. Bar = 200 μ m, tu = tumor. (F) The amount of VEGFC protein in the whole murine liver autopsied at POD 28. ** $p < 0.01$. All the data are expressed as means \pm SD.



S5 Figure Gene expression associated with lymphangiogenesis is not affected by MIP-1 α neutralization in tumor associated macrophages.

The result of microarray analysis is shown in the heat map. We extracted probes for lymphangiogenesis- or microRNA-related genes from probes that had the “P” flag (detected signals) in at least one sample. The criteria for gene regulation were: Z-score ≥ 2.0 and ratio ≥ 1.5 for upregulated genes, and Z-score ≤ -2.0 and ratio ≤ 0.66 for downregulated genes. Microarray data analysis was performed by Cell Innovator Inc. (Fukuoka, Japan, <https://www.cell-innovator.com>). Our data have been uploaded to the Gene Expression Omnibus database (accession number; GSE113235).



S6 Figure Only 1 µg rhVEGFC-administrated mice show significantly expanded CRCLM, compared with 0 ng administered mice.

The gross appearance of colorectal cancer metastasis bearing-liver with/without rhVEGFC autopsied at POD 28. The mice were administrated 0, 0.01, 0.1 or 1 µg rhVEGFC every other day from POD 1 to 10.

Acknowledgements

We thank Jeremy Allen, PhD, from Edanz Group (www.edanzediting.com/ac) for editing a draft of this manuscript.

References

- 1) A. Jemal, F. Bray, M.M. Center, J. Ferlay, E. Ward, D. Forman: Global cancer statistics. *CA: a cancer journal for clinicians* 61: 69-90, 2011.
- 2) J. Leporrier, J. Maurel, L. Chiche, S. Bara, P. Segol, G. Launoy: A population-based study of the incidence, management and prognosis of hepatic metastases from colorectal cancer. *Br J Surg* 93: 465-474, 2006.
- 3) E.K. Abdalla, J.N. Vauthey, L.M. Ellis, V. Ellis, R. Pollock, K.R. Broglio, K. Hess, S.A.: Curley, Recurrence and outcomes following hepatic resection, radiofrequency ablation, and combined resection/ablation for colorectal liver metastases. *Ann Surg* 239: 818-825, 2004.
- 4) M. Koike, K. Yasui, A. Torii, S. Kodama: Prognostic significance of entrapped liver cells in hepatic metastases from colorectal cancer. *Ann Surg* 232: 653-657, 2000.
- 5) I.B. Enquist, Z. Good, A.M. Jubb, G. Fuh, X. Wang, M.R. Junttila, E.L. Jackson, K.G. Leong: Lymph node-independent liver metastasis in a model of metastatic colorectal cancer. *Nat Commun* 5: 3530, 2014.
- 6) P. Carmeliet, R.K. Jain: Molecular mechanisms and clinical applications of angiogenesis. *Nature* 473: 298-307, 2011.
- 7) S.A. Stacker, S.P. Williams, T. Karnezis, R. Shayan, S.B. Fox.: Lymphangiogenesis and lymphatic vessel remodelling in cancer. *Nat Rev Cancer* 14: 159-172, 2014.
- 8) C. Tacconi, C. Correale, A. Gandelli, A. Spinelli, E. Dejana, S. D'Alessio, S. Danese: Vascular endothelial growth factor C disrupts the endothelial lymphatic

- barrier to promote colorectal cancer invasion. *Gastroenterol* 148: 1438-1451, e1438, 2015.
- 9) A. Sasaki, M. Aramaki, K. Kawano, K. Yasuda, M. Inomata, S. Kitano: Prognostic significance of intrahepatic lymphatic invasion in patients with hepatic resection due to metastases from colorectal carcinoma. *Cancer* 95: 105-111, 2002.
 - 10) J.A. de Ridder, N. Knijn, B. Wiering, J.H. de Wilt, I.D. Nagtegaal: Lymphatic Invasion is an Independent Adverse Prognostic Factor in Patients with Colorectal Liver Metastasis. *Ann Surg Oncol* 22 Suppl 3: S638-645, 2015.
 - 11) S. Hirakawa, S. Kodama, R. Kunstfeld, K. Kajiya, L.F. Brown, M. Detmar: VEGF-A induces tumor and sentinel lymph node lymphangiogenesis and promotes lymphatic metastasis. *J Exp Med* 201: 1089-1099, 2005.
 - 12) S. Hirakawa, L.F. Brown, S. Kodama, K. Paavonen, K. Alitalo, M. Detmar: VEGF-C-induced lymphangiogenesis in sentinel lymph nodes promotes tumor metastasis to distant sites. *Blood* 109: 1010-1017, 2007.
 - 13) P. Menten, A. Wuyts, J. Van Damme: Macrophage inflammatory protein-1. *Cytokine Growth Factor Rev* 13: 455-481, 2002.
 - 14) P.N. Siriwardana, T.V. Luong, J. Watkins, H. Turley, M. Ghazaley, K. Gatter, A.L. Harris, D. Hochhauser, B.R. Davidson: Biological and Prognostic Significance of the Morphological Types and Vascular Patterns in Colorectal Liver Metastases (CRLM): Looking Beyond the Tumor Margin. *Medicine* 95: e2924, 2016.
 - 15) W.K. You, B. Sennino, C.W. Williamson, B. Falcon, H. Hashizume, L.C. Yao, D.T. Aftab, D.M. McDonald: VEGF and c-Met blockade amplify angiogenesis inhibition in pancreatic islet cancer. *Cancer Res* 71: 4758-4768, 2011.
 - 16) J.M. Ebos, C.R. Lee, W. Cruz-Munoz, G.A. Bjarnason, J.G. Christensen, R.S. Kerbel: Accelerated metastasis after short-term treatment with a potent inhibitor of tumor angiogenesis. *Cancer cell* 15: 232-239, 2009.
 - 17) T. Tammela, K. Alitalo, Lymphangiogenesis: Molecular mechanisms and future promise. *Cell* 140: 460-476, 2010.
 - 18) K. Alitalo, T. Tammela, T.V. Petrova: Lymphangiogenesis in development and human disease. *Nature* 438: 946-953, 2005.
 - 19) H. Ji, R. Cao, Y. Yang, Y. Zhang, H. Iwamoto, S. Lim, M. Nakamura, P. Andersson, J. Wang, Y. Sun, S. Dissing, X. He, X. Yang, Y. Cao: TNFR1 mediates TNF-alpha-induced tumour lymphangiogenesis and metastasis by modulating VEGF-C-VEGFR3 signalling, *Nat Commun* 5: 4944, 2014.
 - 20) K.L. Hall, L.D. Volk-Draper, M.J. Flister, S. Ran: New model of macrophage acquisition of the lymphatic endothelial phenotype. *PloS one* 7: e31794, 2012.
 - 21) M. Tanaka, Y. Iwakiri, The Hepatic Lymphatic Vascular System: Structure, Function, Markers, and Lymphangiogenesis. *Cell Mol Gastroenterol Hepatol* 2: 733-749, 2016.
 - 22) A.K. Alitalo, S.T. Proulx, S. Karaman, D. Aebischer, S. Martino, M. Jost, N. Schneider, M. Bry, M. Detmar: VEGF-C and VEGF-D blockade inhibits inflammatory skin carcinogenesis. *Cancer Res* 73: 4212-4221, 2013.
 - 23) B. Zhang, Y. Zhang, G. Yao, J. Gao, B. Yang, Y. Zhao, Z. Rao: M2-polarized macrophages promote metastatic behavior of Lewis lung carcinoma cells by inducing vascular endothelial growth factor-C expression. *Clinics (Sao Paulo)* 67: 901-906, 2012.
 - 24) H. Wu, J.B. Xu, Y.L. He, J.J. Peng, X.H. Zhang, C.Q. Chen, W. Li, S.R. Cai: Tumor-associated macrophages promote angiogenesis and lymphangiogenesis of gastric cancer. *J Surg Oncol* 106: 462-468, 2012.
 - 25) G. Kuwahara, H. Nishinakamura, D. Kojima, T. Tashiro, S. Kodama: Vascular endothelial growth factor-C derived from CD11b+ cells induces therapeutic improvements in a murine model of hind limb ischemia. *J Vasc Surg* 57: 1090-1099, 2013.
 - 26) Y. Nakasone, M. Fujimoto, T. Matsushita, Y. Hamaguchi, D.L. Huu, M. Yanaba, S. Sato, K. Takehara, M. Hasegawa: Host-derived MCP-1 and MIP-1alpha regulate protective anti-tumor immunity to localized and metastatic B16 melanoma. *Am J Pathol* 180: 365-374, 2012.
 - 27) Y. Wu, Y.Y. Li, K. Matsushima, T. Baba, N. Mukaida: CCL3-CCR5 axis regulates intratumoral accumulation of leukocytes and fibroblasts and promotes angiogenesis in murine lung metastasis process. *J Immunol* 181: 6384-6393, 2008.
 - 28) Y.Y. Liao, H.C. Tsai, P.Y. Chou, S.W. Wang, H.T. Chen, Y.M. Lin, I.P. Chiang, T.M. Chang, S.K. Hsu, M.C. Chou, C.H. Tang, Y.C. Fong: CCL3 promotes angiogenesis by dysregulation of miR-374b/ VEGF-A axis in human osteosarcoma cells. *Oncotarget* 7: 4310-4325, 2016.
 - 29) M.P. Roberti, J.M. Arriaga, M. Bianchini, H.R. Quinta, A.I. Bravo, E.M. Levy, J. Mordoh, M.M. Barrio: Protein expression changes during human triple negative breast cancer cell line progression to lymph node

- metastasis in a xenografted model in nude mice. *Cancer Biol Ther* 13: 1123-1140, 2012.
- 30) S. Mancardi, E. Vecile, N. Duseti, E. Calvo, G. Stanta, O.R. Burrone, A. Dobrina: Evidence of CXC, CC and C chemokine production by lymphatic endothelial cells. *Immunology* 108: 523-530, 2003.
- 31) S.Y. Kim, J.M. Jeong, S.J. Kim, W. Seo, M.H. Kim, W.M. Choi, W. Yoo, J.H. Lee, Y.R. Shim, H.S. Yi, Y.S. Lee, H.S. Eun, B.S. Lee, K. Chun, S.J. Kang, S.C. Kim, B. Gao, G. Kunos, W.I. Jeong: Pro-inflammatory hepatic macrophages generate ROS through NADPH oxidase 2 via endocytosis of monomeric TLR4-MD2 complex. *Nat Commun* 8: 2247, 2017.
- 32) F. Tacke, H.W. Zimmermann: Macrophage heterogeneity in liver injury and fibrosis. *J Hepatol* 60: 1090-1096, 2014.
- 33) M.P. Holt, L. Cheng, C. Ju: Identification and characterization of infiltrating macrophages in acetaminophen-induced liver injury. *J Leuko Biol* 84: 1410-1421, 2008.
- 34) T. Kitamura, T. Fujishita, P. Loetscher, L. Revesz, H. Hashida, S. Kizaka-Kondoh, M. Aoki, M.M. Taketo: Inactivation of chemokine (C-C motif) receptor 1 (CCR1) suppresses colon cancer liver metastasis by blocking accumulation of immature myeloid cells in a mouse model. *Proc Natl Acad Sci USA* 107: 13063-13068, 2010.
- 35) E. Farmaki, V. Kaza, A.G. Papavassiliou, I. Chatzistamou, H. Kiaris: Induction of the MCP chemokine cluster cascade in the periphery by cancer cell-derived Ccl3. *Cancer Lett* 389: 49-58, 2017.
- 36) Y. Tanabe, S. Sasaki, N. Mukaida, T. Baba: Blockade of the chemokine receptor, CCR5, reduces the growth of orthotopically injected colon cancer cells via limiting cancer-associated fibroblast accumulation. *Oncotarget* 7: 48335-48345, 2016.
- 37) P. Carmeliet, V. Ferreira, G. Breier, S. Pollefeyt, L. Kieckens, M. Gertsenstein, M. Fahrig, A. Vandenhoeck, K. Harpal, C. Eberhardt, C. Declercq, J. Pawling, L. Moons, D. Collen, W. Risau, A. Nagy: Abnormal blood vessel development and lethality in embryos lacking a single VEGF allele. *Nature* 380: 435-439, 1996.
- 38) M. Lohela, M. Bry, T. Tammela, K. Alitalo: VEGFs and receptors involved in angiogenesis versus lymphangiogenesis. *Curr Opin Cell Biol* 21: 154-165, 2009.
- 39) V. Joukov, V. Kumar, T. Sorsa, E. Arighi, H. Weich, O. Saksela, K. Alitalo: A recombinant mutant vascular endothelial growth factor-C that has lost vascular endothelial growth factor receptor-2 binding, activation, and vascular permeability activities. *J Biol Chem* 273: 6599-6602, 1998.
- 40) J. Stachura, M. Wachowska, W.W. Kilarski, E. Guc, J. Golab, A. Muchowicz: The dual role of tumor lymphatic vessels in dissemination of metastases and immune response development. *Oncoimmunology* 5: e1182278, 2016.
- 41) T. Karpanen, M. Egeblad, M.J. Karkkainen, H. Kubo, S. Yla-Herttuala, M. Jaattela, K. Alitalo: Vascular endothelial growth factor C promotes tumor lymphangiogenesis and intralymphatic tumor growth. *Cancer Res* 61: 1786-1790, 2001.
- 42) Y. He, I. Rajantie, K. Pajusola, M. Jeltsch, T. Holopainen, S. Yla-Herttuala, T. Harding, K. Jooss, T. Takahashi, K. Alitalo: Vascular endothelial cell growth factor receptor 3-mediated activation of lymphatic endothelium is crucial for tumor cell entry and spread via lymphatic vessels. *Cancer Res* 65: 4739-4746, 2005.
- 43) G. Procopio, E. Verzoni, I. Testa, N. Nicolai, R. Salvioni, F. Debraud: Experience with sorafenib in the treatment of advanced renal cell carcinoma. *Ther Adv Urol* 4: 303-313, 2012.
- 44) Y. Kodera, Y. Katanasaka, Y. Kitamura, H. Tsuda, K. Nishio, T. Tamura, F. Koizumi: Sunitinib inhibits lymphatic endothelial cell functions and lymph node metastasis in a breast cancer model through inhibition of vascular endothelial growth factor receptor 3. *Breast Cancer* 13: R6-6, 2011.
- 45) S.L. Davis, S.G. Eckhardt, W.A. Messersmith, A. Jimeno: The development of regorafenib and its current and potential future role in cancer therapy. *Drugs Today (Barc)* 49: 105-115, 2013.
- 46) A. Grothey, E. Van Cutsem, A. Sobrero, S. Siena, A. Falcone, M. Ychou, Y. Humblet, O. Bouche, L. Mineur, C. Barone, A. Adenis, J. Tabernero, T. Yoshino, H.J. Lenz, R.M. Goldberg, D.J. Sargent, F. Cihon, L. Cupit, A. Wagner, D. Laurent: Regorafenib monotherapy for previously treated metastatic colorectal cancer (CORRECT): an international, multicentre, randomised, placebo-controlled, phase 3 trial. *Lancet* 381: 303-312, 2013.
- 47) M. Tampellini, C. Sonetto, G.V. Scagliotti: Novel anti-angiogenic therapeutic strategies in colorectal cancer. *Expert Opin Investig Drugs* 25: 507-520, 2016.

(平成 30. 9. 3 受付, 平成 30. 10. 11 受理)

「The authors declare no conflict of interest.」